Journal of Babylon University/ Engineering Sciences / No.(2)/ Vol.(21): 2013

Experimental and Theoretical investigation of Aerodynamics Characteristics of flow Around a Bus

Emad Shukri ali *University of Babylon*
Mawlood Anwer Faris *Alsuwayra Technical institute*
Ali Hamza *Ministry of Oil*

Abstract

In the present work the aerodynamic characteristics of a bus was studied. Flow analyses was carried out assuming two dimensional, steady incompressible and viscous. The effect of speed and yaw angle variation were investigated separately. Experimental and theoretical investigations were carried out. A bus model of 1:20 scale ratio was used for experimental testes. A wooden bus model was made with smooth surfaces to simulate the prototype.

The tests were carried out in a low speed wind tunnel, the air speed was varied from 14.5 m/s to 24.5 m/s and yaw angle from 0^o to 15°.

A package program (Ansys 5.4) was used to carry out the theoretical study. This gave a good ability to calculate the pressure and velocity distribution and sketching the eddies in the near wake behind the bus model. It was found that increasing the yaw angle increases the drag and pressure coefficients .At air speed equals to 14.5 m/s the difference in the pressure coefficient in the flow direction C_P(front-rear) varies from 0.05 at $Q=0^o$ to -0.055 at $Q=10^o$, .For the same condition the drag coefficient varies from 0.72 to 0.76.

The comparison made between the experimental results, and some experimental published data showed a good agreement. The results obtained by Ansys 5.4 program for the specific configureuration were compared with the present experimental work and they showed a reasonable agreement .

الخلاصة

في البحث الحالي تم دراسة الخواص الديناهوائية للحافلة. تم تحليل الجريان على اساس ثلاثي الابعاد ومستقر ولا انضغاطي ولزج. تمت دراسة تأثير تغير السرعة وزواية الانحراف لكل سطح من السطوح بشكل منفصل.

اجريت دراسة عملية ونظرية. تم استخدام نموذج حافلة بمقياس رسم (1 : 20) للاختبارات العملية، تم تصنيع نموذج خشبي للحافلة بسطوح ملساء مشابهة لسطوح الحافلة اجريت الاختبارات في نفق هوائي ذي سرعة منخفضة. تم تغيير سرعة الهواء في الاختبارات من (14.5 م/ ثا) الى (25.5 م/ ثا) وتم تغيير. الانحراف من 0 – 15 درجة واستخدمِ برنامج الانسزللدراسة النظرية.ان استخدام هذا البرنامج يعطي امكانية جيدة لحساب توزيع الضغط والسرعة ورسم الدوامات المتولدة عند الاثر خلف الحافلة. وقد وجد ان الزيادة بزاوية الانحراف تؤدي الى زيادة بالاعاقة والضغط حيث وجد عند سرعة14,5 م/ثا ان معامل الضغط يتراوح بين 0,05 عند زاوية انحراف تساوي صفرا الى –0,055 عند الزاوية 10 ولنفس السرعة وان الاعاقة تتراوح بين 0,72 الى 0,76 ان المقارنة بين النتائج العملية والنتائج العملية لابحاث سابقة كانت متطابقة بشكل جيد وكذلك ان المقرنة بين النتائج العمليةو النظرية لهذا البحث اعطت تقارب معقول.

Nomenclature

Symbol	Meaning	Units
A	Body arbitrary cross section area	m^2
A_P	Prototype frontal cross sectional area	m^2
A_{fb}	Projected fore-body area	m^2
A_b	Projected base area	m^2
A_w	Wetted surfaces area parallel to freestream direction excluding under-body	m^2
C_p	Pressure coefficient	--
C_D	Drag coefficient	--
C_f	Skin friction coefficient	--
L1	Front length	m
L2	Base length	m

L3	Roof length	m
P_s	Static pressure	N/m^2
P_∞	Freestream pressure	N/m^2
$P_{tot.}$	Total pressure	N/m^2
R_e	Reynolds number	--
U_∞	Air velocity in freestream	m/s
τ	Shear wall	N/m^2

Greek Symbols

θ	Yaw angle	deg.
ε	Overall blockage factor	--
ρ	Density	kg/m^3

2. Introduction

After a quick development in road vehicles, and increasing the distances between the cities, the dependence on the buses for traveling of passengers increased. Buses became the cheapest tool for transferring and have the ability to overcome the increasing in the passenger number. Therefore, the need increased for the production of more comfortable buses which have speed of 120 km/hr.(Lajos & Prezler, 1986).

In 1970's, after the oil crisis, the need was appeared to produce a road vehicles with low fuel consumption, also this need was appeared for decreasing air pollution by decreasing fuel burnt for this purpose (decreasing fuel burnt) the researches take two paths; the first path is the production of vehicles which have low resistance for air force (development the aerodynamic characteristics). The second one is the production of engines with high efficiency (consumed low quantity of fuel).(Mercker, 1986)

The present study concentrates on the effect of some aerodynamics parameters such as pressure distribution on all surfaces, velocity, and shear distribution on the surfaces parallel to the flow. The underbody and the clearance between model and the ground are not considered in the present work.

The effect of edges (sharp or rounded) on shear stress, flow pattern and separation and re-attachment in the beginning of parallel surfaces were investigated. Fuel economy has become a very important aspect of automobiles manufactured today. The aerodynamics group has direct input in the fuel economy results via a rule of thumb, which states that 10% reduction in drag can result in about 3 % increase in fuel economy. (Lajos & Prezler, 1986). Therefore, there are many experimentally papers done by using wind tunnel, and theoretical works done by using some computational technique to predict the aerodynamic characteristics.

Ahmed (1981) studied the wake structures of typical automobile shapes experimentally. He points out that the amount of drag experienced by vehicle is related to the structure of the flow in its wake. The near wakes of the fastback, notchback and Estate models contain separation bubbles attached to the vehicle base.

Lajos and Prezler (1986) studied the effect of moving ground simulation on the flow past bus models by using rotating wheels model to investigate the mud deposition on the body. They indicate that the structure of the wake may be controlled by the simultaneity of effect of changes in underbody flow and in skin friction on the ground surface.

Saathoff, and Melbourne,(1989) investigated the occurrence of large negative peak pressure near the leading edge of sharp-edged bluff bodies. And they indicate that the increase in free-stream turbulence reduces the size of the separation bubble and thus reduces the minimum value of the mean pressure coefficient.

Tamas Lajos (2001) studied the reduction of the aerodynamic drag and mud deposition at buses. It can be noted that reduction of aerodynamic drag and mud deposition is important tasks of bus body development. Depending on the rounding up of the leading edges, boundary layer separation occurs and a ring shaped separation bubble surrounds the front part of the body. The flow rate of under- body flow depends mainly on the existence of boundary layer separation on the lower horizontal leading edge and the size of separation bubble at the inlet of the under-body gap.

3.The Scope of the Present Work

The aerodynamic drag of buses is not investigated directly by any one of the previous theses. Some theses study the aerodynamic drag of tractor-trailer or trucks and mud deposition of buses. The effect of add-on devices or typical configure ration of bodies like road vehicles is studied. The effect of some factors as moving ground, solid boundaries of test section, and the shape of the test section is also investigated. Therefore, in the present study the aerodynamic drag of buses is investigated experimentally and theoretically.

4.Experimental Work

The given configureuration model whose scale (1:20) is made and tested in a wind tunnel having (0.45m* 0.45m) test section .A schematic diagram of the test rig is shown in figure. (A). Bus model is made of wood with few details used for experimental test(Figure.B). The tests objective of the present work is to study the aerodynamic properties of the (bus) which is carried out at a low speed wind tunnel. The test is repeated many times with different values for the air speed and the yaw angle_The model is made of six wood plates compacted together to make a space inside the model for the pressure probes. The model scale is 1:20 to permit that the blockage area ratio is not to exceed 10%.. The model simulates the front and rear bumper, the sides and roof curvature, the shape of fore-body and base-body, the tiers and wheel arches. The other details, such as front and rear lights, mirrors, front and side windows and the under body components are neglected. Multi-Tube Manometer: which has 36 tubes used to measure the pressure. The test is carried out for velocity whose range (14.5,19.5,24.5 m/s) and the yaw angle that varies from (0^o to 15^o) step 5^o.

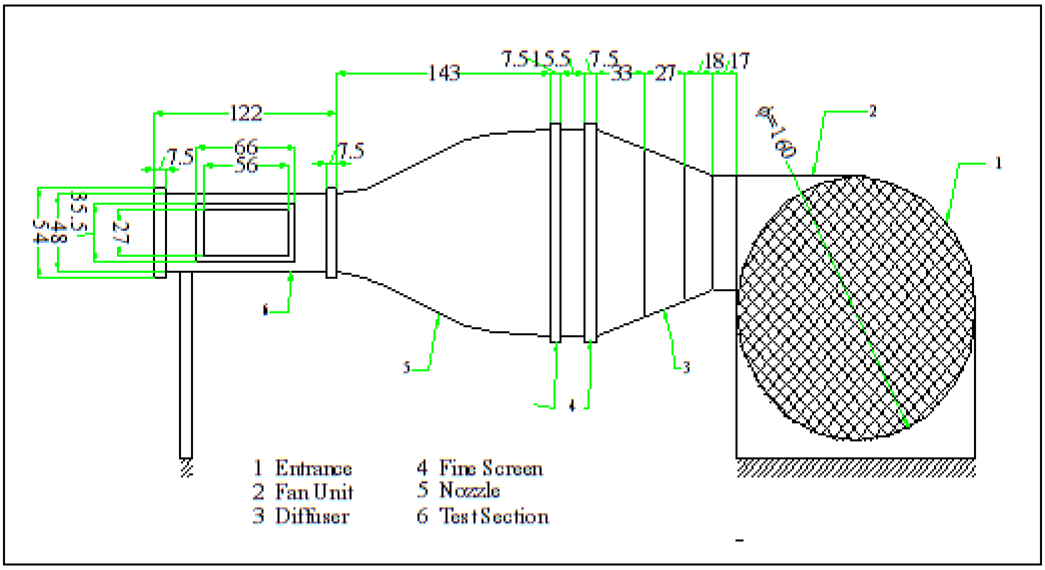

Figure. A / Test rig wind tunnel

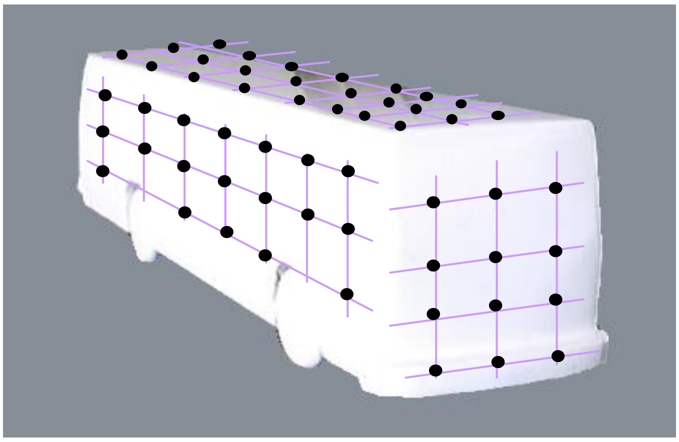

5.Theoretical Work

The theoretical results presented in this chapter are obtained by Ansys 5.4 program. This package program solves the fluid flow problems by solving momentum and continuity equations. The k–ε (two-equation) model is used to overcome the turbulence in the flow. By using finite element technique, this program analyzes the flow field around the bus model. There are many types of meshing controls. The boundary condition can be changed to cover all the actual boundary condition. The regular areas created by a solid model must be meshed one after another. To mesh any area the lines of that area must be divided firstly. The boundary condition must be applied on the lines. The bus velocity is simulated by applying velocity varies by varying the velocity of the air in the duct entrance. The velocity in the model lines must be set zero to simulate the solid walls. Also upper and lower lines of the duct are given zero velocity where the wind tunnel has a closed test section.

The governing equations solved in the theoretical work are the continuity and momentum equations in two dimensions.(Robert & Alan, 1998).

$$\frac{\partial \rho}{\partial t} + \frac{\partial(\rho V_x)}{\partial x} + \frac{\partial(\rho V_y)}{\partial y} = 0 \qquad (1)$$

$$\rho(\frac{\partial u}{\partial t}+q.\nabla u)=\rho X_X-\frac{\partial P}{\partial x}+\frac{\partial}{\partial x}\{\mu_e[2\frac{\partial u}{\partial x}-\frac{2}{3}(\nabla.q)]\}+\frac{\partial}{\partial y}[\mu_e(\frac{\partial u}{\partial y}+\frac{\partial v}{\partial x})] \qquad (2)$$

$$\rho(\frac{\partial v}{\partial t}+q.\nabla v)=\rho X_y-\frac{\partial P}{\partial y}+\frac{\partial}{\partial y}\{\mu_e[2\frac{\partial v}{\partial y}-\frac{2}{3}(\nabla.q)]\}+\frac{\partial}{\partial x}[\mu_e(\frac{\partial v}{\partial x}+\frac{\partial u}{\partial y})] \qquad (3)$$

Where:

V_x, V_y = component of the velocity vector in the x, and y direction

g_x g_y =components of acceleration due to gravity

ρ = density

μ_e = effective viscosity

Some terms must be eliminated when solving the problem. For the steady state analysis the time dependent terms must be eliminated. The density enters as a constant value. Therefore the final form of the continuity and momentum equations is as follows:

$$\frac{\partial V_x}{\partial x}+\frac{\partial V_y}{\partial y}=0 \qquad (4)$$

$$\rho(u\frac{\partial u}{\partial x}+v\frac{\partial u}{\partial y})=-\frac{\partial p}{\partial x}+\frac{\partial}{\partial x}\left(\mu_e\frac{\partial u}{\partial x}\right)+\frac{\partial}{\partial y}\left(\mu_e\frac{\partial u}{\partial y}\right) \qquad (5)$$

$$\rho(u\frac{\partial v}{\partial x}+v\frac{\partial v}{\partial y})=-\frac{\partial p}{\partial y}+\frac{\partial}{\partial x}\left(\mu_e\frac{\partial v}{\partial x}\right)+\frac{\partial}{\partial y}\left(\mu_e\frac{\partial v}{\partial y}\right) \qquad (6)$$

For the turbulent case the effective viscosity (Ground Vehicles Drag, 2001):

$$\mu_e=\mu+\mu_t \qquad (7)$$

where μ: laminar viscosity (fluid property)

μ_t: turbulent viscosity

The two equations (k-ε) turbulent model is used to evaluate the turbulent viscosity through the expression

$$\mu_t=c_\mu\rho\frac{k^2}{\varepsilon} \qquad (8)$$

where k: turbulent kinetic energy

ε: turbulent kinetic energy dissipation rate

6-Results and Discussion

6.1 Theoretical results : The pressure coefficient is the ratio between the pressure force (local pressure minus the freestream pressure) and the dynamic pressure force. $C_p=\dfrac{P_n-P_\infty}{\frac{1}{2}\rho U_\infty{}^2}$

If the value of the pressure coefficient positive the local air velocity is greater than the freestream velocity, while if it is negative the local air velocity less than the freestream velocity. However If the value of the pressure coefficient equals zero the local air velocity equals the freestream velocity. Figure (1) shows that the range of the pressure coefficient variation in the frontal area of the bus ,.The curve shown that the value of pressure coefficient starts from zero at the lower point (Y/L1 = 0) and, reaches (C_p = 0.06). Then it is decreased gradually to reach (C_p = -0.37) at (Y/L1=1), Similarly provided that the separation is absent.

Figure (2) shows the value of the pressure coefficient in the rare side of the bus where the negative side from (Y/L2 = 0) to (Y/L2 =1). The air velocity at the nodes near the rear line is greater than that of freestream. The increase in air velocity in the wake of the bus is due to the presence of a suction flow in the zone behind the bus. Where the flow that comes from the underbody raised and that comes from over-body is lowered to feed the suction zone (wake). Therefore in the wake there are many vortices in different directions. The value of the pressure coefficient at the lower edge (Y/L2=0) is (C_p=-0.66) and it is decreased. The value of the pressure coefficient is sometimes decreased and sometimes increased randomly due to the effect of vortices in the wake. The shape and the strength of the vortices in the wake is also dependent on the shape of the rear model.

Figure (3) shows the streamline through the wind tunnel for the theoretical work explain the change in the value of the stream function [$\psi = -\partial u / \partial y$]. Figure (4) shows the resultant velocity [$V_{sum} = \sqrt{u^2 + v^2}$] through the wind tunnel for the theoretical work which explain the change in the value of the resultant velocity, and shows the velocity in the x-direction [$V_x = u$] through the wind tunnel for the theoretical work the gray gradient explain the change in the value of the velocity. Figures (5), and (6) show the velocity vectors ahead and behind the model.

6.2-Experimental Results :

Figures from (7- to 14) explain the pressure coefficient distribution on the front, rear, right side, left side and roof of bus for different yaw angles (θ= 0, 5, 10, 15) and for the range of bus model velocity (U=14.5, 19.5, 24.5 m/s). The probes distributed in 2D for each surface are converted to 1D in centerline of this surface. Figures (7 & 8) show the pressure coefficient distribution on the rear and right surface of bus for different yaw angles except for (U=19.5 m/s). Figure 7 shows that the pressure coefficient is negative in all points of rear surface, and the maximum value in the upper edge of the rear part which decreases towards lower direction to point (Y/L2=0.25) where (C_p= -0.65, -0.58, -0.52 and -0.47) for (θ=0^o,5^o,10^o,15^o) respectively, and then increases slightly.

There is a wake behind the bus. The flow under-body is min. compared with the flow of the over-body; therefore, the pressure coefficient reaches the smallest value. The suction pressure decreases towards the upper edge of the rear surface, and pressure coefficient increases significantly.

According to figure.(8) the pressure coefficient in the front edge is negative because of the separation of the flow over rounded corners between front and right sides. The flow after this edge can be reversed and cause pressure on this surface. Soon after the separation is started quickly re-attacking to the surface. Therefore, the pressure is increasing on the surface and the same behavior noticed for the pressure coefficient. When the yaw angle varies from (0° to 5°) the starting value of pressure coefficient decreases from (C_p = -0.021) to (C_p = -0.027) and then increases quickly for the first curve. However, for the yaw angle (θ = 10°) the curve behavior is similar to (θ = 5°) curve. For (θ = 15°) the flow is divided into two parts by the effect of rounded corner. Figure (9) show the pressure coefficient distribution on the roof of the bus for different yaw angles. In this figure the pressure coefficient value starts from a positive value and increases until (X/L3=0.3). This indicates that for leading edge the eddies presence above the rounded edge causes no flow separation.

Figure (9), show the pressure coefficient distribution on the roof of the bus for different yaw angles. In this figure. where (θ=0°, 5°) respectively the pressure coefficient value starts from a positive value and increases until (X/L_3=0.3). This indicates that for leading edge the eddies presence above the rounded edge causes no flow separation.

Figure (10) shows that the maximum value of pressure coefficient near the middle point of the front face reaches (C_p=0.45) which decreases towards upper until it reaches (C_p=0.25) and decreases toward lower until it reaches (C_p=0.075). But when yaw angle ($\theta=5^o$) the curve is displaced towards positive side. In the middle point when (Y/L_1= 0.5) the pressure coefficient (C_p=0.7) and (C_p=0.5) for upper point.

The maximum value of pressure coefficient indicates that at this point the flow is approximately stagnant and the dynamic pressure reaches zero .In the upper and lower edges the flow is accelerated and the pressure coefficient decreases.

Figure (11) show the pressure coefficient on right side bus for different yaw angles at velocity of 24.5 m/s. In this figure. the first curve (θ = 0°) the pressure coefficient value starts from (C_p = -0.13), and then increases sharply and approximately reaches (C_p = 0.62) for the rest of the curve, but for yaw angle (θ = 5°) the starting value is (C_p = -0.39) then it increases quickly to reach a value (C_p = 0.68) at (X/L_3 = 0.25) , The three curves are close to each other. This indicates that for high velocity the effect of cross wind is the same for different yaw angles for the side exposed to cross wind.

Figures (12) show the pressure coefficient distribution on the left side of the bus for different yaw angles. In this figure. the first curve yaw angle (θ = 0°). The behavior of this curve in the leading edge of the flow is separated from the surface and there is a reverse flow that causes a suction pressure on the surface. Therefore, the pressure coefficient has a negative value. After some distance in the flow direction, the flow re-attacks the surface and the pressure coefficient suddenly increases (C_p =0.65) where (X/L_3 = 0.25).

Figures (13 and 14) show the shear stress distribution on the roof, and right sides of the bus where yaw angle ranging (θ = 0º, 5º, 10º, 15º) for bus velocity (U=24.5 m/s). The probes of measuring total and static pressure for every surface are distributed in the centerline of the surface. The shear stress is measured in the laminar sublayer of the turbulent flow, and the negative value of shear stress is physically without meaning. The shear in the opposite direction indicates mathematically that there is a separation flow on the surface. .In figure 14 the shear stress in the leading edge starts from positive value and then it is decreased to zero. For this point there is no separation of flow $[\tau = 0]$ where the flow re-attacks the surface again in the same location. This behavior comes from eddies near the wall effect.

Aerodynamic drag can be defined as the force that resists the motion of bodies immersed in a fluid. The drag of vehicles results from two types of force such as a shear force and a pressure force, which are acting on the body. The drag caused by shear is often called skin-friction drag. The drag caused by the pressure force is called form drag. Figure (15) shows the variation of total drag coefficient of bus for different yaw angles and velocities. In this there are positive and negative yawing angles. The two sides of the bus are symmetric, in that the right side of the positive yaw angle is the left side for the negative yaw angle and vice versa.

The drag level is minimum when the yaw angle (θ=0°) [no yawing condition] and then increased by increasing the yaw angle in the positive side and decreasing angle in the negative side. Increasing in the total drag coefficient comes from increasing the drag force on the body of the bus. The frontal area of the vehicle exposed to pressure is increased by increasing the yaw angle limit to increasing drag that results from increasing yawing.

Figure (16) shows the power required to overcome the aerodynamic drag of the bus. This figure is important to get some useful information about the quantity of fuel consumed by the bus. Before selecting the engine used with this type of bus the quantity of power consumed for the drag must be known. The rest power of the engine of the bus is used for driving the bus. This consumed power is linearly proportional to the drag and it is directly proportional to the cubic velocity of the bus.

This Figure shows the lowest level of power consumed for the lowest velocity (U=52.2 km/hr) when yaw angle (θ=0°).The drag force and the power are calculated as follows:

$$F_{DP} = \frac{1}{2} C_D \ \rho U_P^2 A_P$$

$$P_P = F_{DP} U_P$$

7- Conclusions

1. The maximum value of the pressure coefficient occur in the location where the flow is slow. This occurs clearly near the middle of the bus front.
2. The value of the pressure coefficient in the area behind the bus is always negative because there is a suction pressure on the rear part of the surface of the bus.
3. There is a suction pressure due to the separation of the boundary layer from the roof surface of the bus and lowering the pressure coefficient to a negative value in the bus front.
4. Increasing the Reynolds number causes the increase in the drag coefficient and finally, increasing the power consumed to resist the drag exerted on the bus.
5. Increasing the yaw angle causes the same effect of increasing the bus speed.

8-References

Ahemd, S.R.“An Experimental Study of the Wake Structures of Typical Automobile Shapes” -Journal of Wind Engineering and Industrial Aerodynamics Vol. 9, (1981), pp. 49-62

Ground Vehicles Drag” -Aerodynamic Drag of Road Vehicles.htm (2001).

Lajos, T. “Simultaneous Reduction of Aerodynamic Drag and Mud Deposition a Buses” (2001)

Lajos, T. and Prezler . “Effect of Moving Ground Simulation on The flow Past Bus Models” -Journal of Wind Engineering and Industrial Aerodynamics Vol. 22, (1986), pp. 271-277

Mercker, E. “A Blockage Correction for Automotive testing in a Wind Tunnel with Closed Test Section “ -Journal of Wind Engineering and Industrial Aerodynamics Vol. 22 (1986) pp. 149-167

Robert Fox, W. and Alan McDonald, T. “Introduction of Fluid Mechanics CH.7 “ 5th Edition August, 1998 John Wiley

Saathoff, P.J. and Melbourne, W.H. “The generation of Peak Pressure in Separated/Re-attaching Flows” -Journal of Wind Engineering and Industrial Aerodynamics Vol. 32 ,(1989), pp. 121-134

Templin, J.T. and Raimondo, S. “Experimental Evaluation of Test Section Boundary Interference Effects in Road Vehicles Test in Wind Tunnel” -Journal of Wind Engineering and Industrial Aerodynamics Vol. 22 (1986) pp. 129-148.

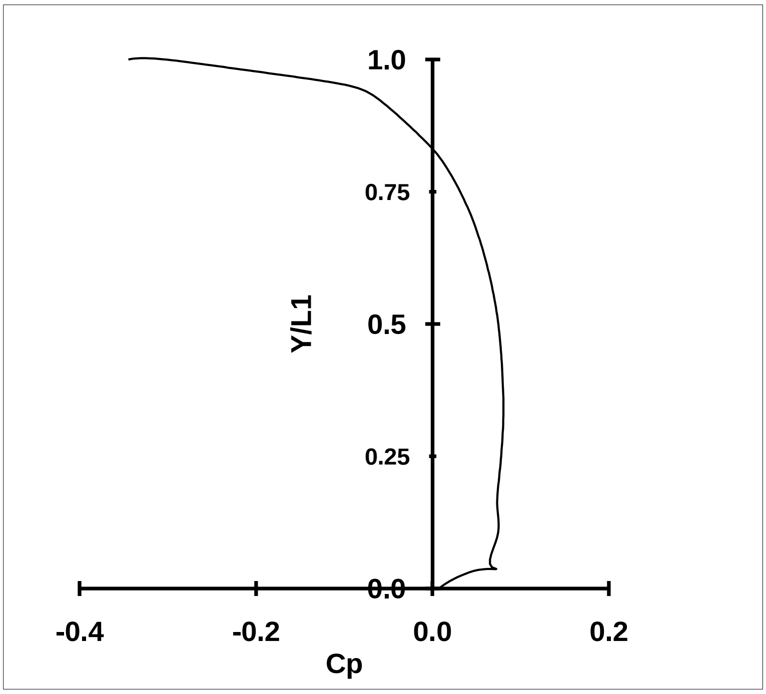

Fig.(1) Pressure Coefficient Distrbution ver. Dimensionless Distance on Front Bus (Velocity=24.5 m/s Yaw Angle=0)

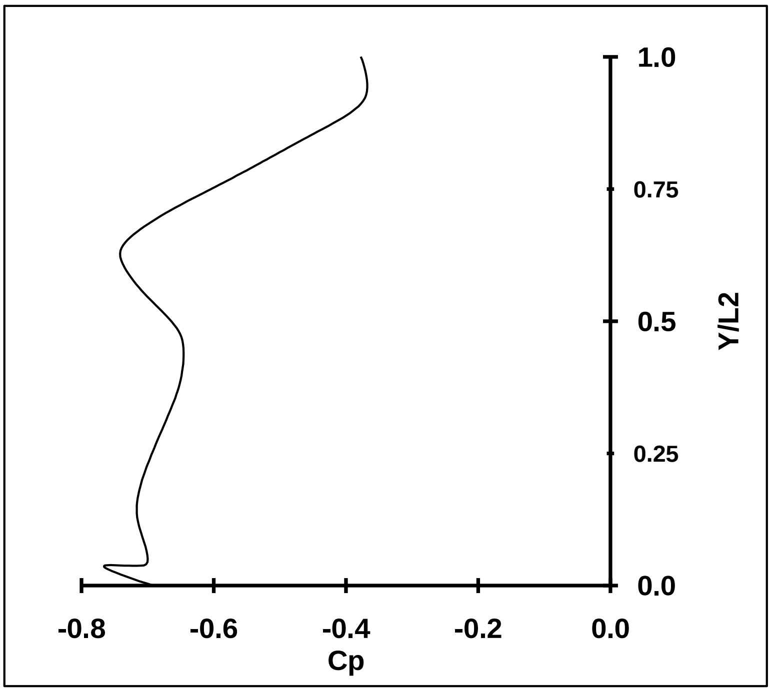

Fig(2) Pressure Coefficient Distrbution ver. Dimensionless Distance on Rear Bus (Velocity=24.5 m/s Yaw Angle=0)

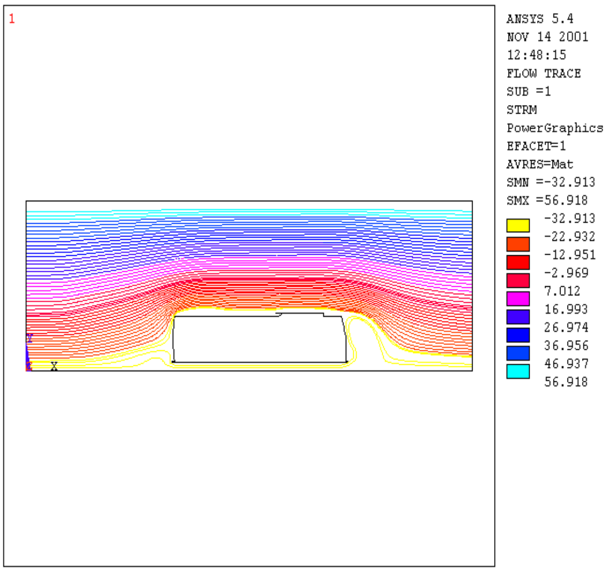

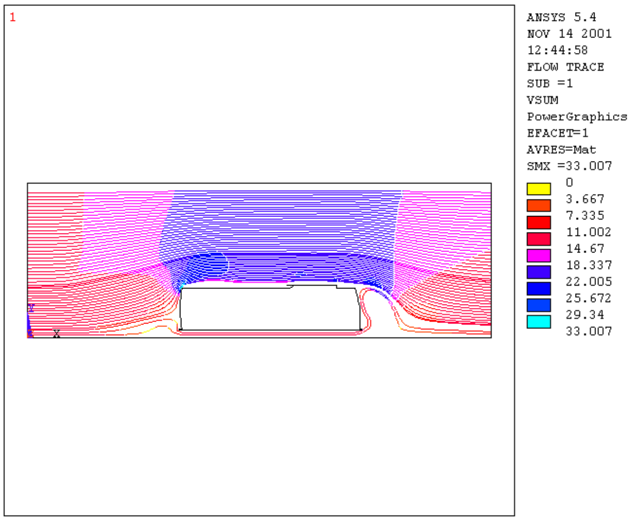

Figure (3) Stream lines through the tunnel

Figure (4) Vsum through the tunnel

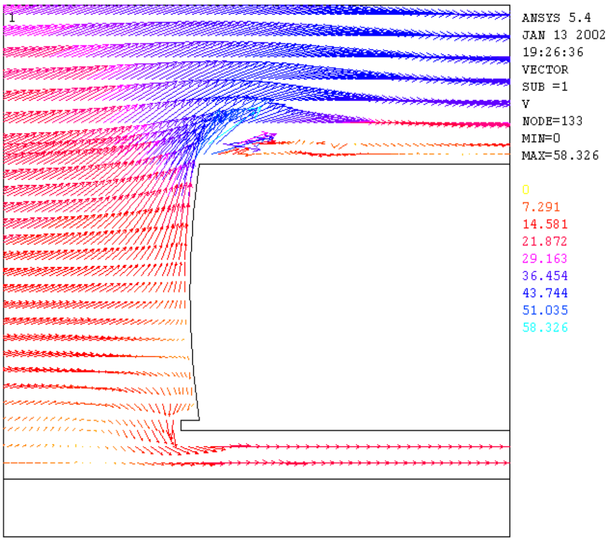

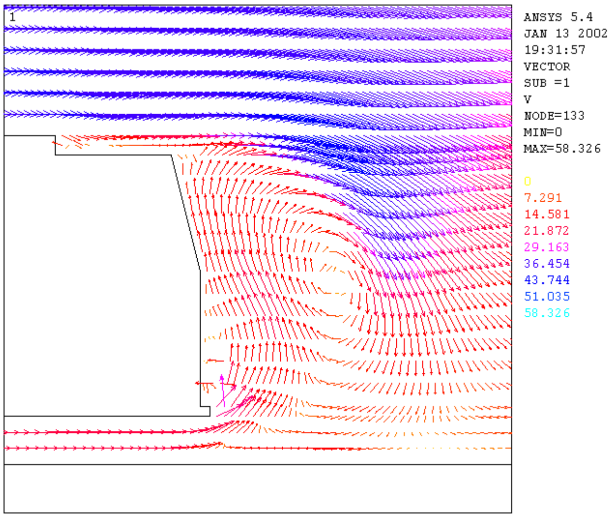

Figure (5) Velocity Vectors Ahead the Model

Figure (6) Velocity Vectors Behind the Model

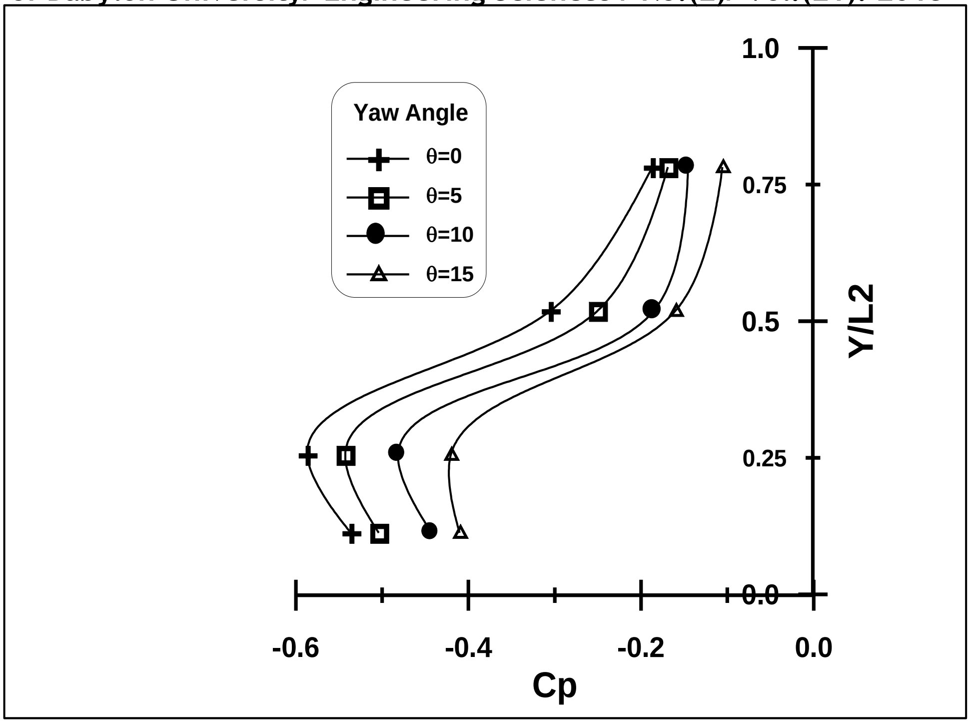

Fig.(7) Prssure Coifficient Distrbution ver.Dimensionless Distance on Rear of Bus (Velocity=19.5 m/s Yaw Angle=0,5,10,15)

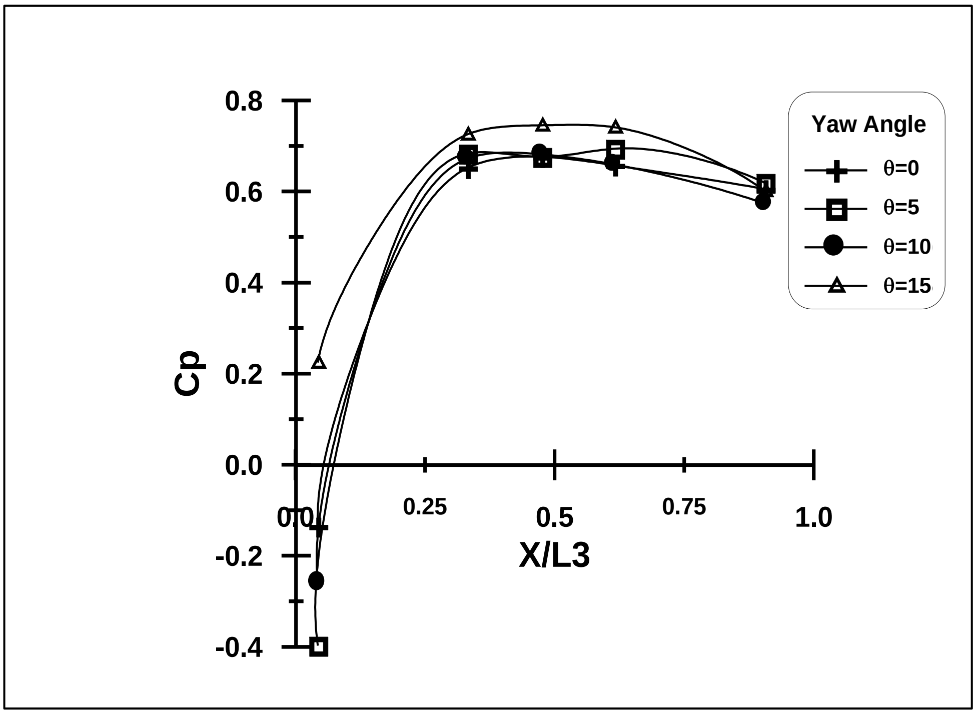

Fig.(8) Prssure Coifficient Distrbution ver. Dimensionless Distance on Right Side of Bus (Velocity=19.5 m/s Yaw Angle=0,5,10,15)

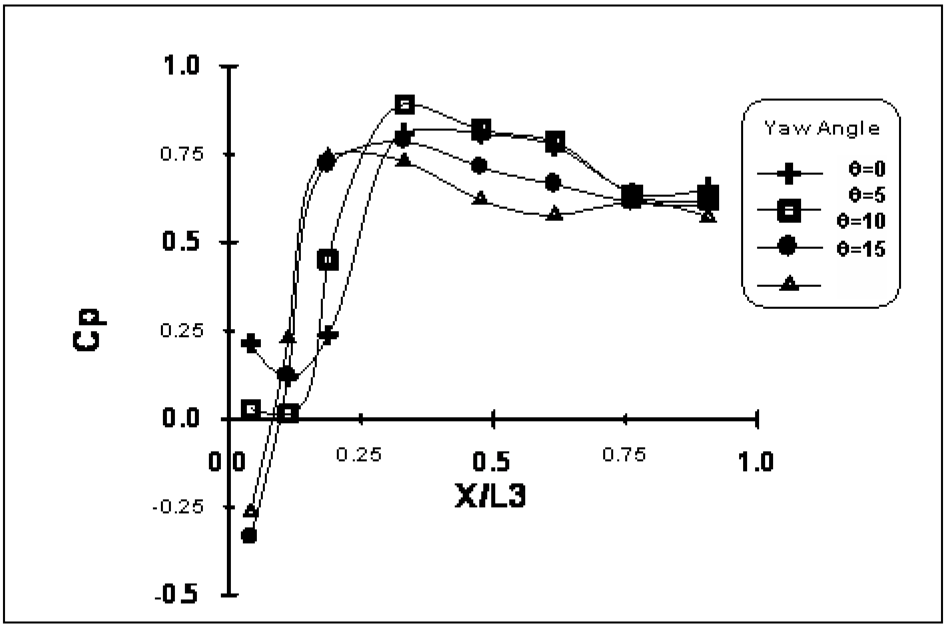

Figure(9) pressure coefficient distribution verse dimensionless distances on Roof of the bus (V= 14.5 m/s , Yaw angle =o. 5 . 10 . 15)

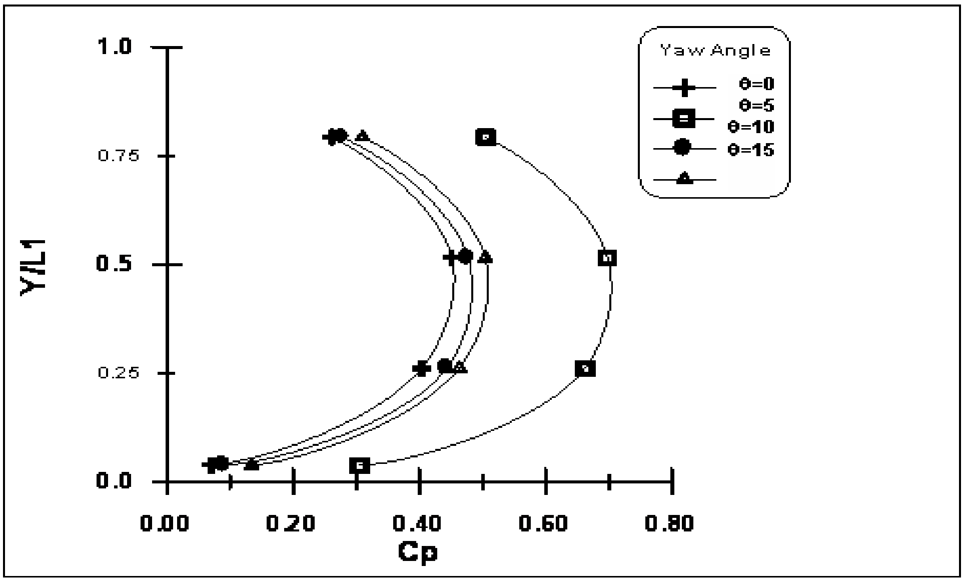

Figure(10) pressure coefficient distribution verse dimensionless distances on front of the bus (V= 14.5 m/s , Yaw angle =o. 5 . 10 . 15)

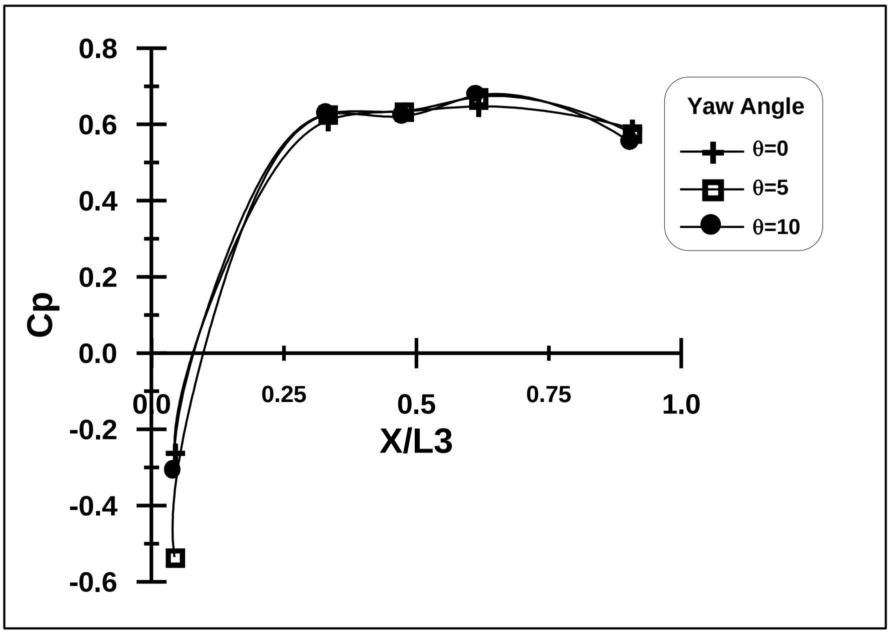

Fig. (11)) Prssure Coifficient Distrbution ver.Dimensionless Distance on Right Side of Bus (Velocity=24.5 m/s Yaw Angle=0,5,10)

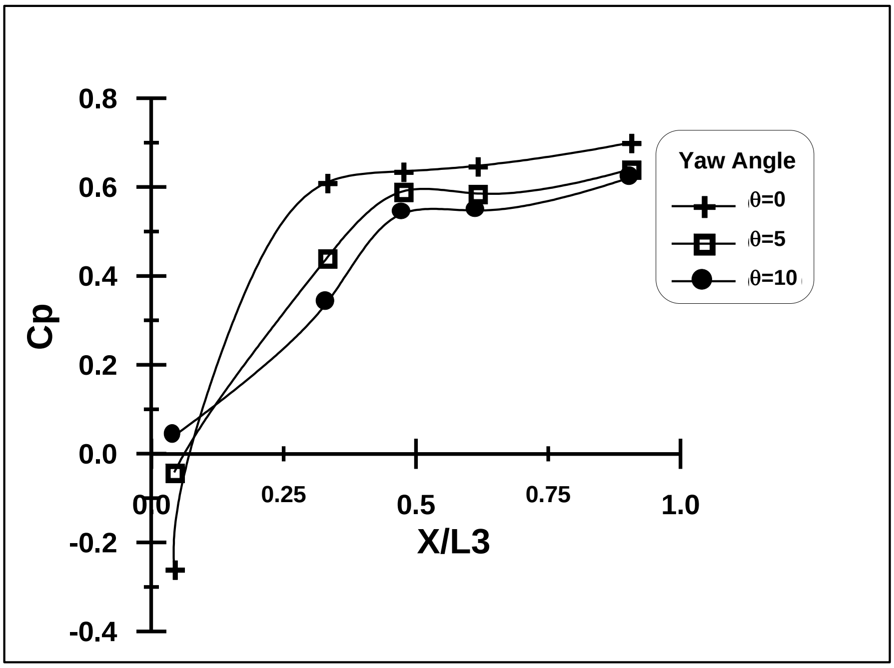

Fig. (12)) Prssure Coifficient Distrbution ver. Dimensionless Distance on Lift Side of Bus(Velocity=24.5 m/s Yaw Angle=0,5,10)

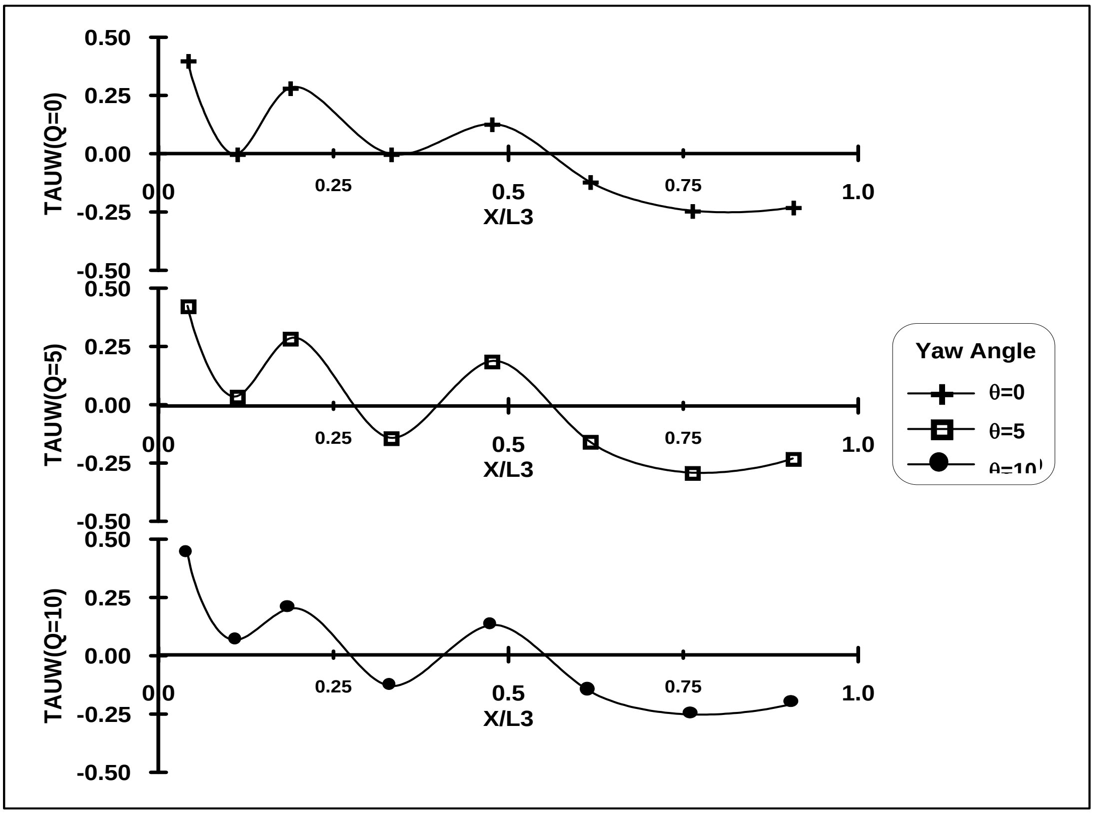

Fig.(13) Vareation of Shear Wall (TAUW) ver. Yaw Angle on Roof of Bus (Velocity=24.5 m/s Yaw Angle=0,5,10,15)

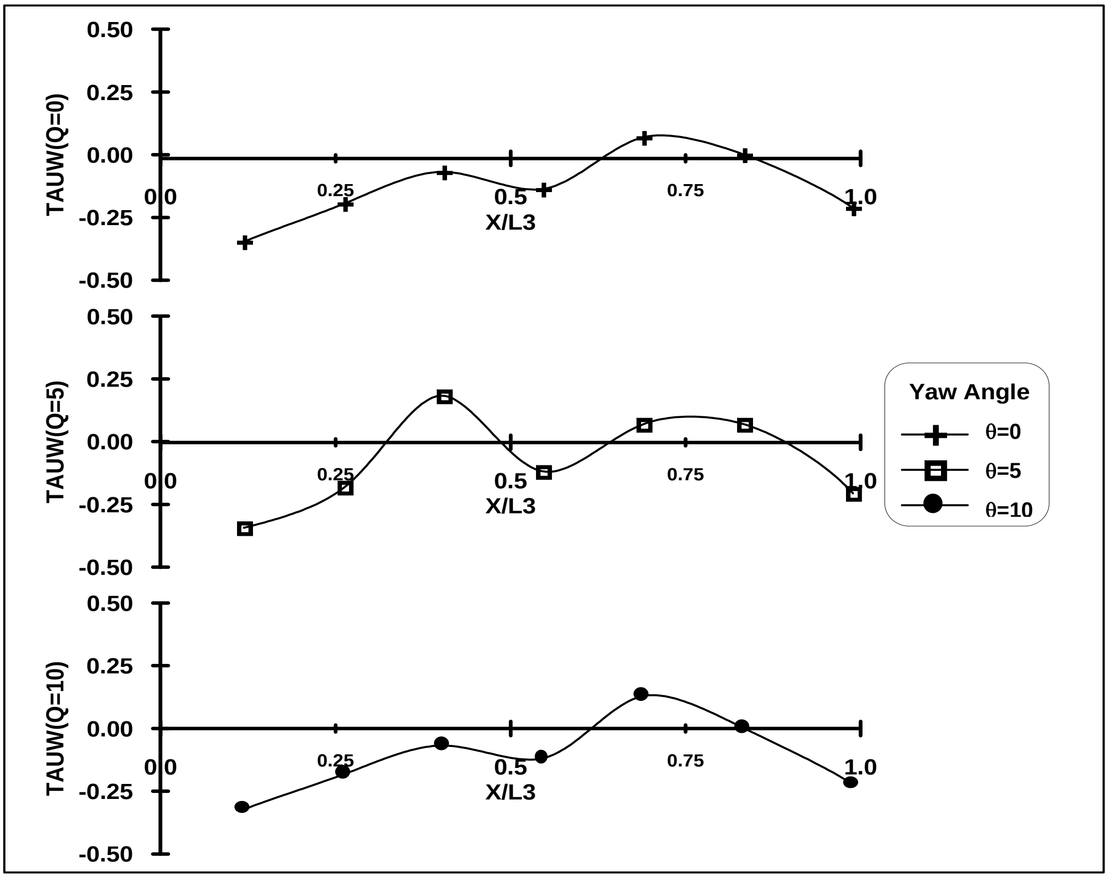

Fig.(14) Vareation of Shear Wall (TAUW) ver. Yaw Angle on Right Side of Bus (Velocity=24.5 m/s Yaw Angle=0,5,10)

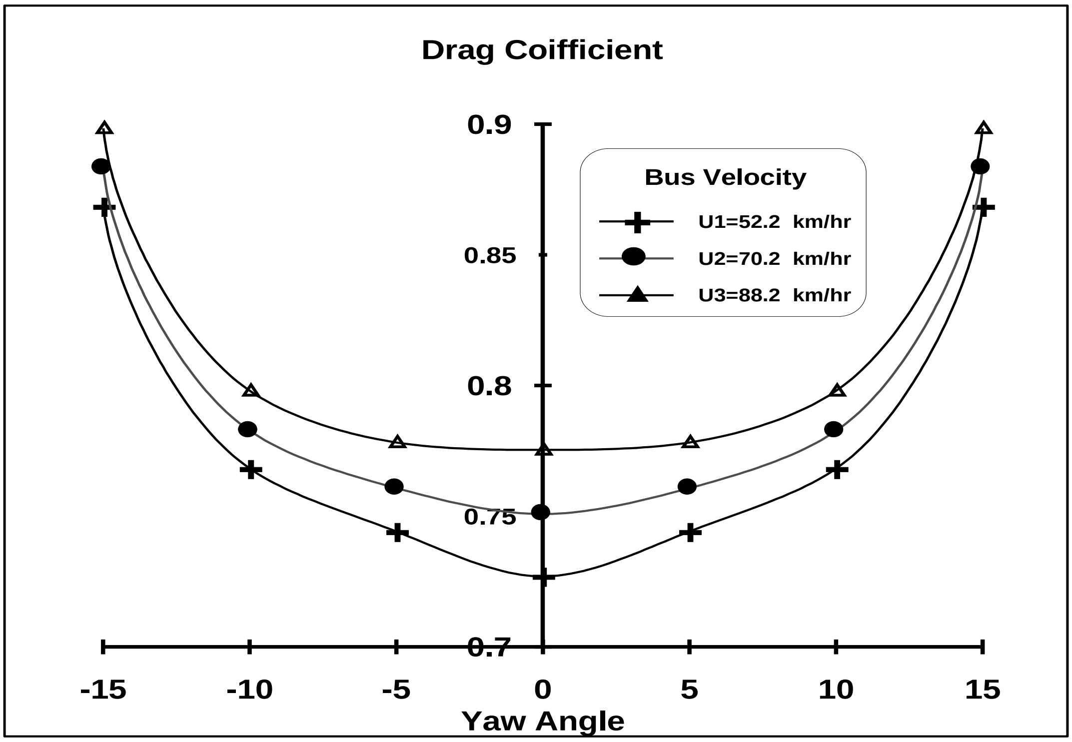

Fig.(15) Vareation of Total Drag Coifficient of Bus ver. Yaw Angle for Different Bus Velocity

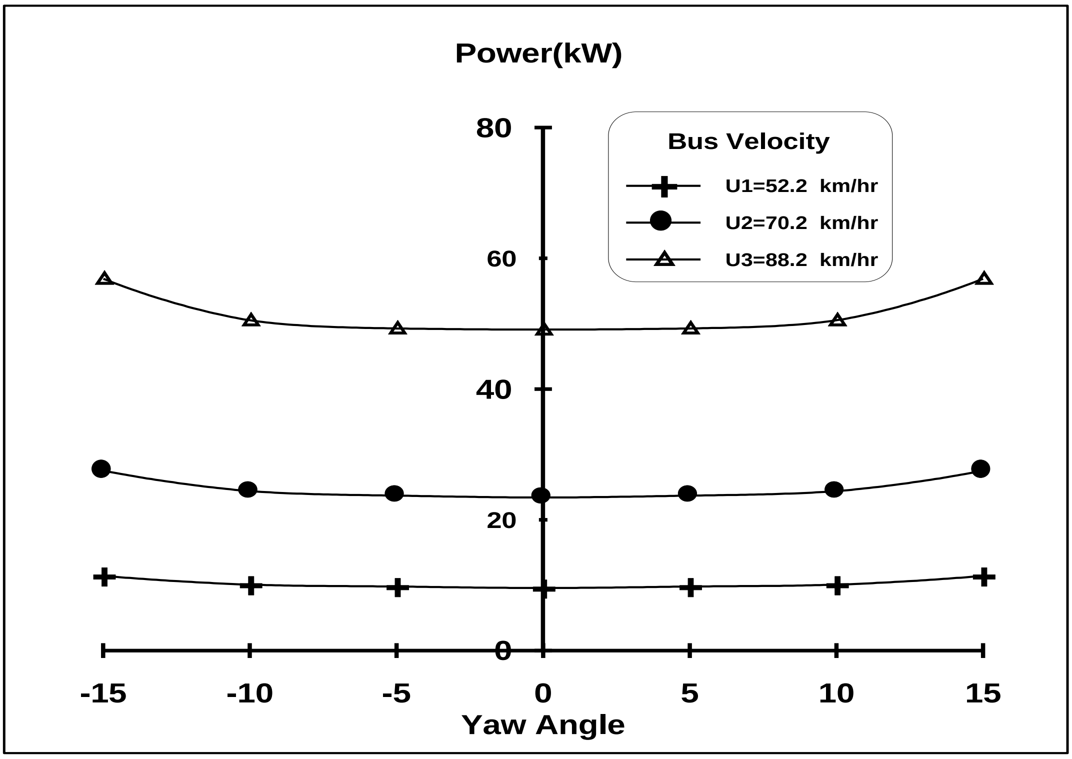

Fig. (16) Power Consumed by Aerodynamic Drag ver. Yaw Angle for Different Bus Velocity